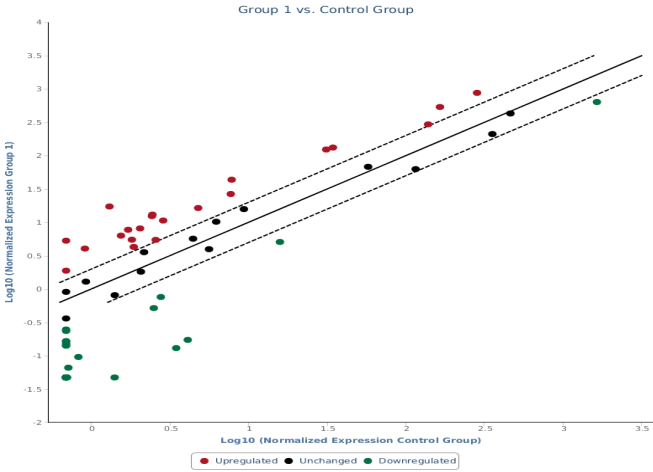


A

Inflammation	Regulation of Acute-Phase Response	Regulation of Cytokine Metabolism	Regulation of Cytokine Receptors	Regulation of Cytokine	Regulation of Humoral Immune Response
hsa-miR-106b-5p hsa-miR-15b-5p hsa-miR-16-5p hsa-miR-17-5p hsa-miR-20a-5p hsa-miR-23b-3p hsa-miR-98-5p hsa-miR-181a-5p hsa-miR-181b-5p hsa-miR-181c-5p hsa-miR-19b-3p	hsa-let-7f-5p hsa-let-7g-5p hsa-miR-106b-5p hsa-miR-125a-5p hsa-miR-17-5p hsa-miR-20a-5p hsa-miR-20b-5p hsa-miR-21-5p hsa-miR-29b-3p hsa-miR-29c-3p hsa-miR-374a-5p hsa-miR-454-3p hsa-miR-98-5p hsa-miR-144-3p hsa-miR-101-3p hsa-let-7a-5p hsa-miR-130a-3p hsa-miR-130b-3p hsa-miR-202-3p hsa-miR-301a-3p hsa-miR-410-3p hsa-miR-449a hsa-miR-548d-3p	hsa-let-7f-5p hsa-let-7g-5p hsa-miR-125a-5p hsa-miR-15b-5p hsa-miR-16-5p hsa-miR-181a-5p hsa-miR-195-5p hsa-miR-23a-3p hsa-miR-23b-3p hsa-miR-30c-5p hsa-miR-23b-3p hsa-miR-30c-5p hsa-miR-30d-5p hsa-miR-30d-5p hsa-miR-374a-5p hsa-miR-424-5p hsa-miR-454-3p hsa-miR-9-5p hsa-miR-98-5p hsa-let-7a-5p hsa-miR-130a-3p hsa-miR-130b-3p hsa-miR-15a-5p hsa-miR-181b-5p hsa-miR-181c-5p hsa-miR-19b-3p hsa-miR-202-3p hsa-miR-301a-3p hsa-miR-302a-3p hsa-miR-302c-3p hsa-miR-410-3p hsa-miR-449a hsa-miR-543	hsa-let-7f-5p; hsa-let-7g-5p hsa-miR-106b-5p; hsa-miR-125a-5p hsa-miR-15b-5p; hsa-miR-16-5p hsa-miR-17-5p; hsa-miR-195-5p hsa-miR-20a-5p; hsa-miR-20b-5p hsa-miR-21-5p; hsa-miR-23a-3p hsa-miR-23b-3p; hsa-miR-29b-3p hsa-miR-29c-3p; hsa-miR-30c-5p hsa-miR-30d-5p; hsa-miR-424-5p hsa-miR-98-5p; hsa-miR-454-3p hsa-miR-9-5p hsa-let-7a-5p; hsa-miR-15a-5p hsa-miR-19b-3p; hsa-miR-202-3p hsa-miR-656-3p; hsa-miR-130a-3p hsa-miR-130b-3p; hsa-miR-211-5p hsa-miR-301a-3p; hsa-miR-548d-3p	hsa-let-7a-5p; hsa-miR-15a-5p hsa-miR-19b-3p; hsa-miR-202-3p hsa-miR-656-3p; hsa-miR-130a-3p hsa-miR-130b-3p; hsa-miR-211-5p hsa-miR-301a-3p; hsa-miR-548d-3p	hsa-let-7f-5p hsa-let-7g-5p hsa-miR-106b-5p hsa-miR-125a-5p hsa-miR-15b-5p hsa-miR-16-5p hsa-miR-17-5p hsa-miR-195-5p hsa-miR-20a-5p hsa-miR-20b-5p hsa-miR-21-5p hsa-miR-23a-3p hsa-miR-23b-3p hsa-miR-29b-3p hsa-miR-29c-3p hsa-miR-30c-5p hsa-miR-30d-5p hsa-miR-424-5p hsa-miR-454-3p hsa-miR-9-5p hsa-miR-98-5p hsa-let-7a-5p hsa-miR-130a-3p hsa-miR-130b-3p hsa-miR-15a-5p hsa-miR-181b-5p hsa-miR-181c-5p hsa-miR-19b-3p hsa-miR-202-3p hsa-miR-301a-3p hsa-miR-302a-3p hsa-miR-302c-3p hsa-miR-410-3p hsa-miR-449a hsa-miR-543
Autoimmunity	hsa-let-7f-5p hsa-miR-16-5p hsa-miR-17-5p hsa-miR-20a-5p hsa-miR-23a-3p hsa-miR-23b-3p hsa-miR-29c-3p hsa-miR-181a-5p hsa-miR-181b-5p hsa-miR-301a-3p	hsa-let-7f-5p hsa-miR-130a-3p hsa-miR-130b-3p hsa-miR-15a-5p hsa-miR-181b-5p hsa-miR-181c-5p hsa-miR-19b-3p hsa-miR-202-3p hsa-miR-301a-3p hsa-miR-302a-3p hsa-miR-302c-3p hsa-miR-410-3p hsa-miR-449a hsa-miR-543	hsa-miR-381-3p hsa-miR-449a	hsa-miR-181a-5p hsa-miR-374a-5p hsa-miR-15a-5p hsa-miR-181b-5p hsa-miR-181c-5p hsa-miR-302a-3p hsa-miR-302c-3p hsa-miR-410-3p hsa-miR-543 hsa-miR-301b-3p hsa-miR-144-3p hsa-miR-101-3p	hsa-miR-181a-5p hsa-miR-374a-5p hsa-miR-98-5p hsa-miR-181a-5p hsa-miR-374a-5p hsa-let-7a-5p hsa-miR-15a-5p hsa-miR-19b-3p hsa-miR-202-3p hsa-miR-656-3p hsa-miR-181b-5p hsa-miR-181c-5p hsa-miR-302a-3p hsa-miR-302c-3p hsa-miR-410-3p hsa-miR-543
	Innate & Adaptive Immunity				
	hsa-miR-17-5p hsa-miR-20a-5p hsa-miR-9-5p hsa-miR-181a-5p hsa-miR-19b-3p				

B



C

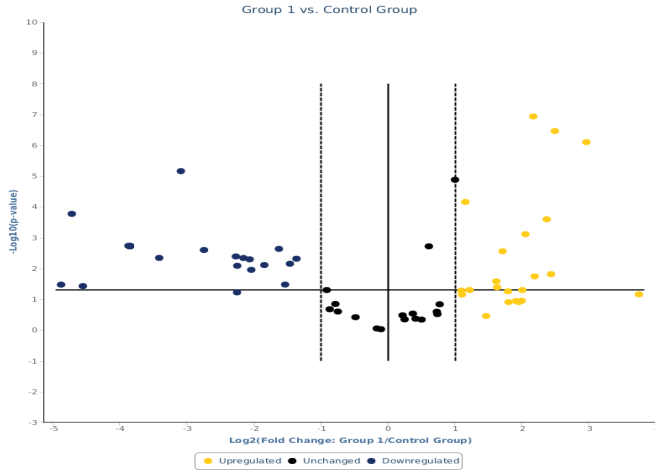


Figure S1

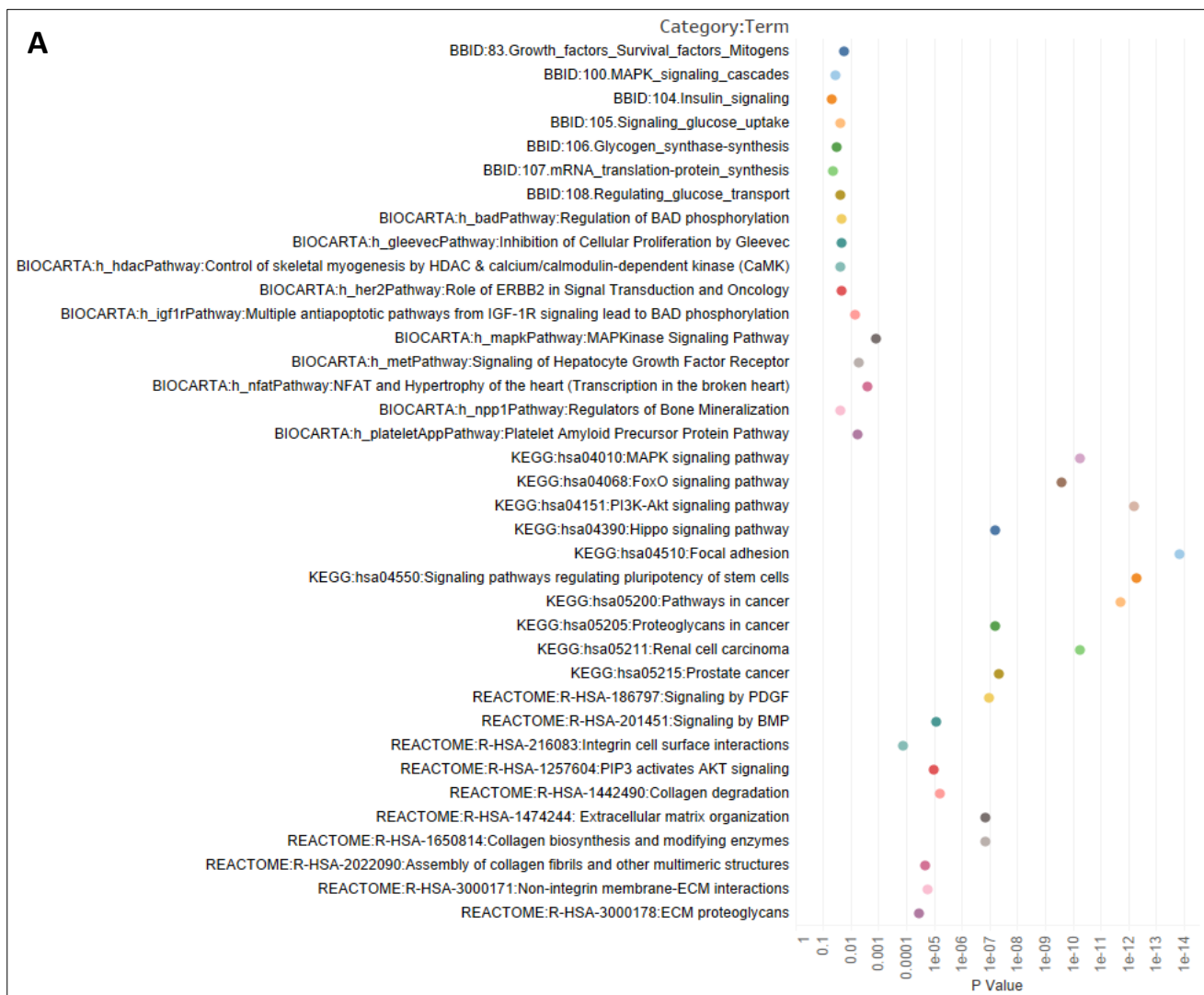
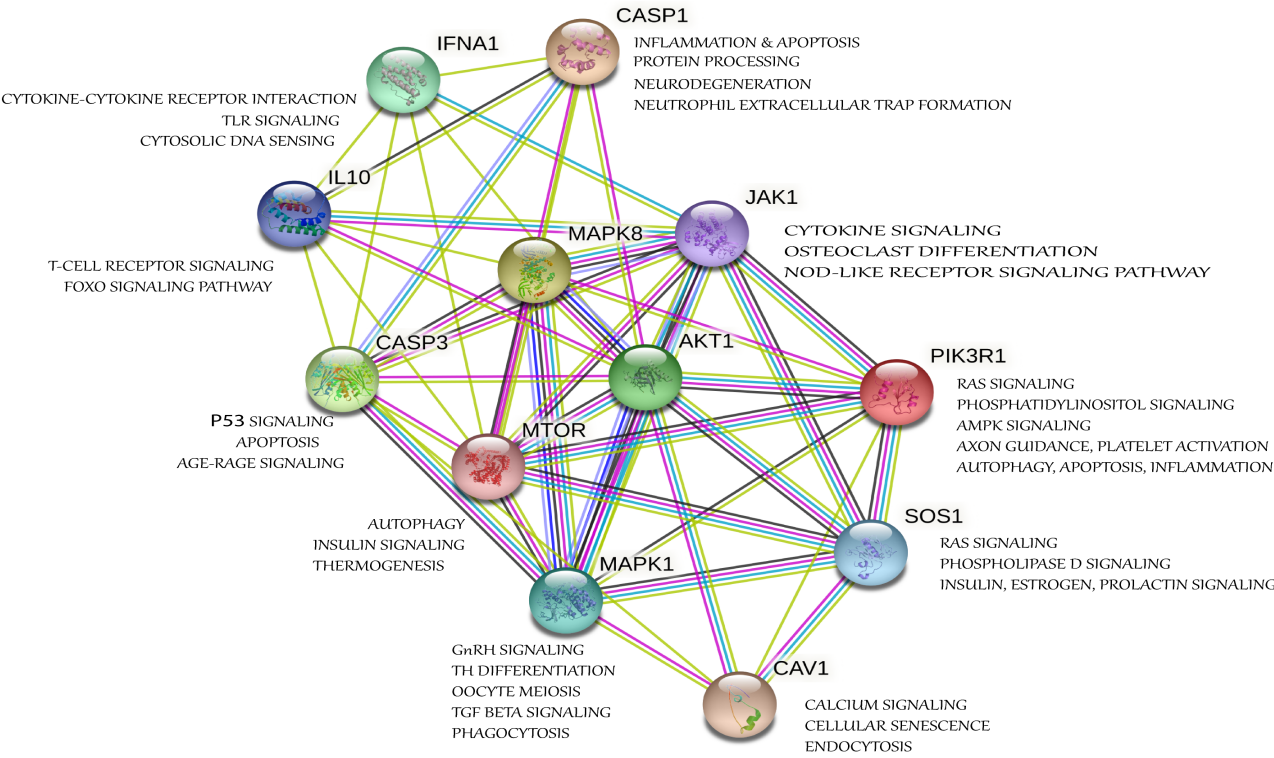
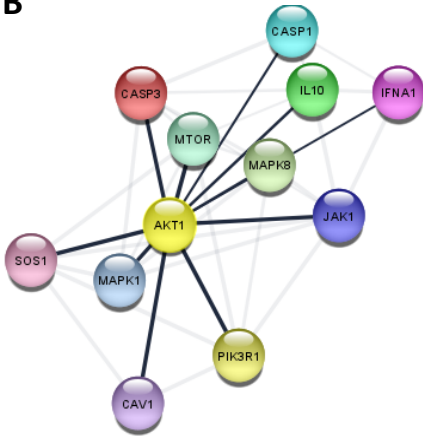


Figure S2

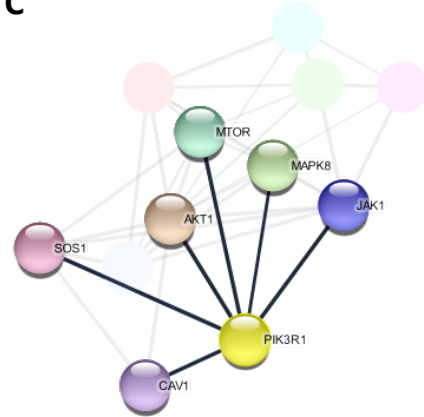
A



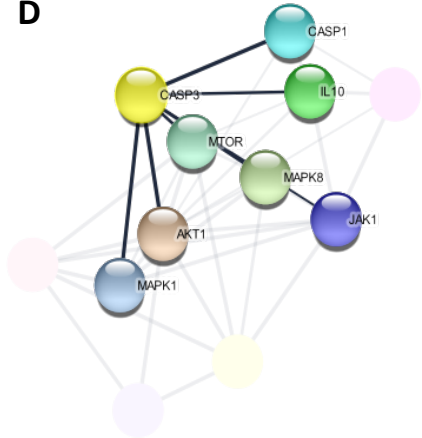
B



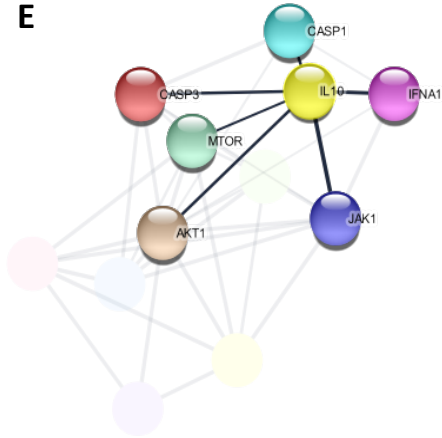
C



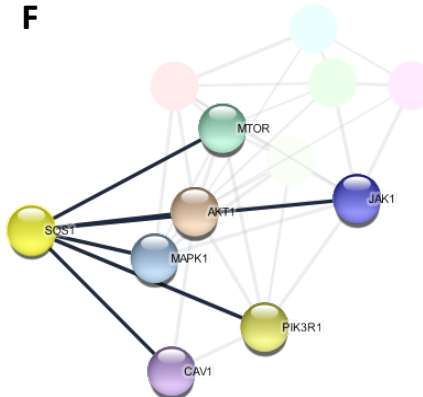
D



E



F



G

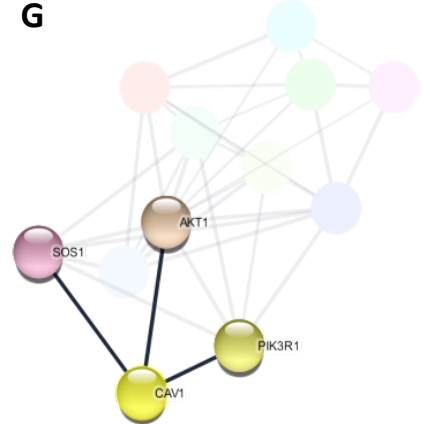
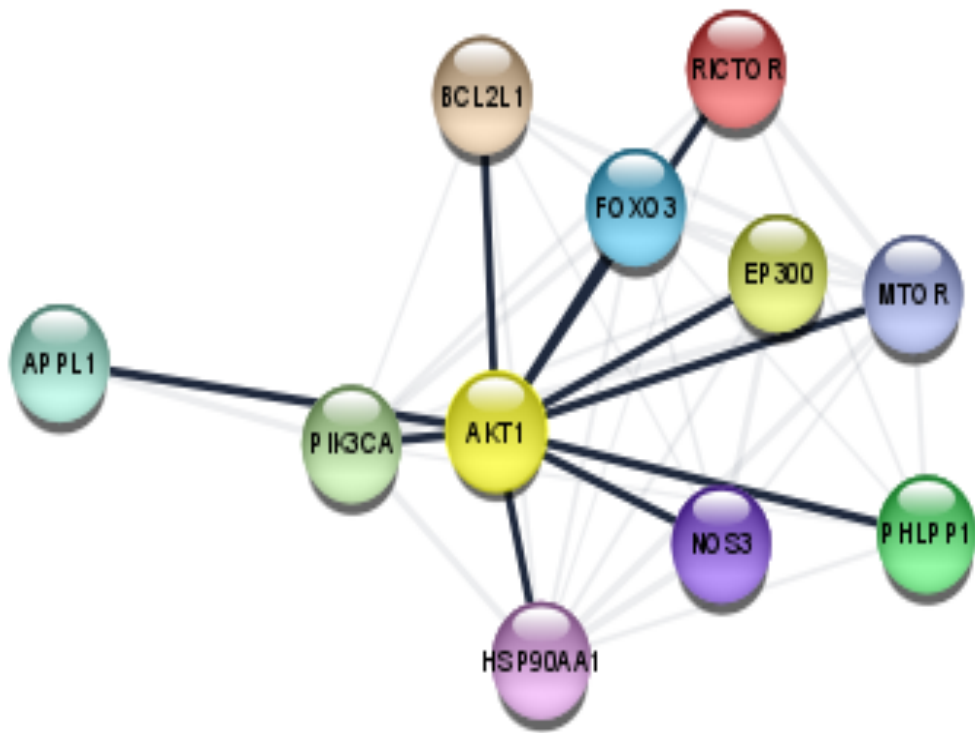


Figure S3

A



B

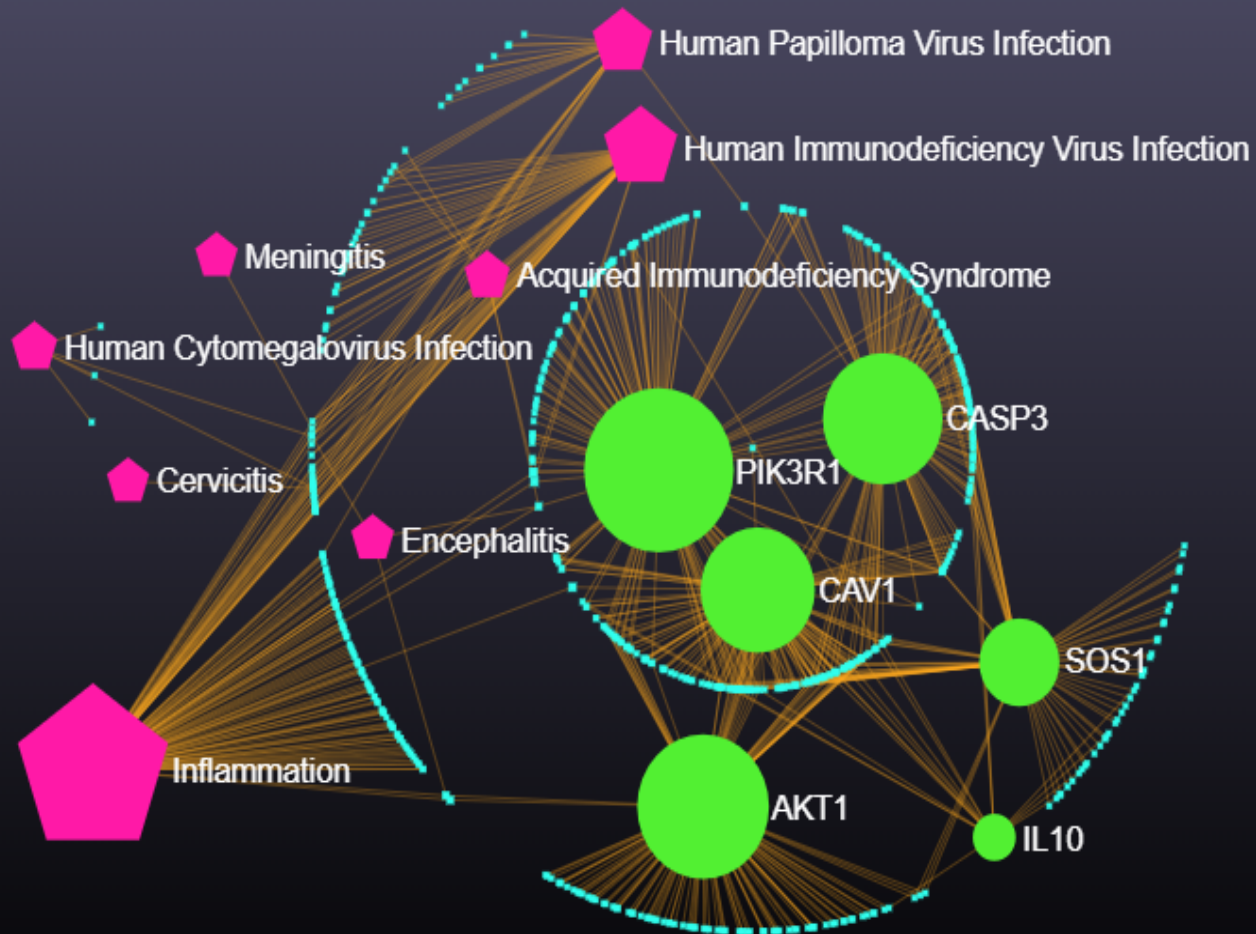


Figure S4

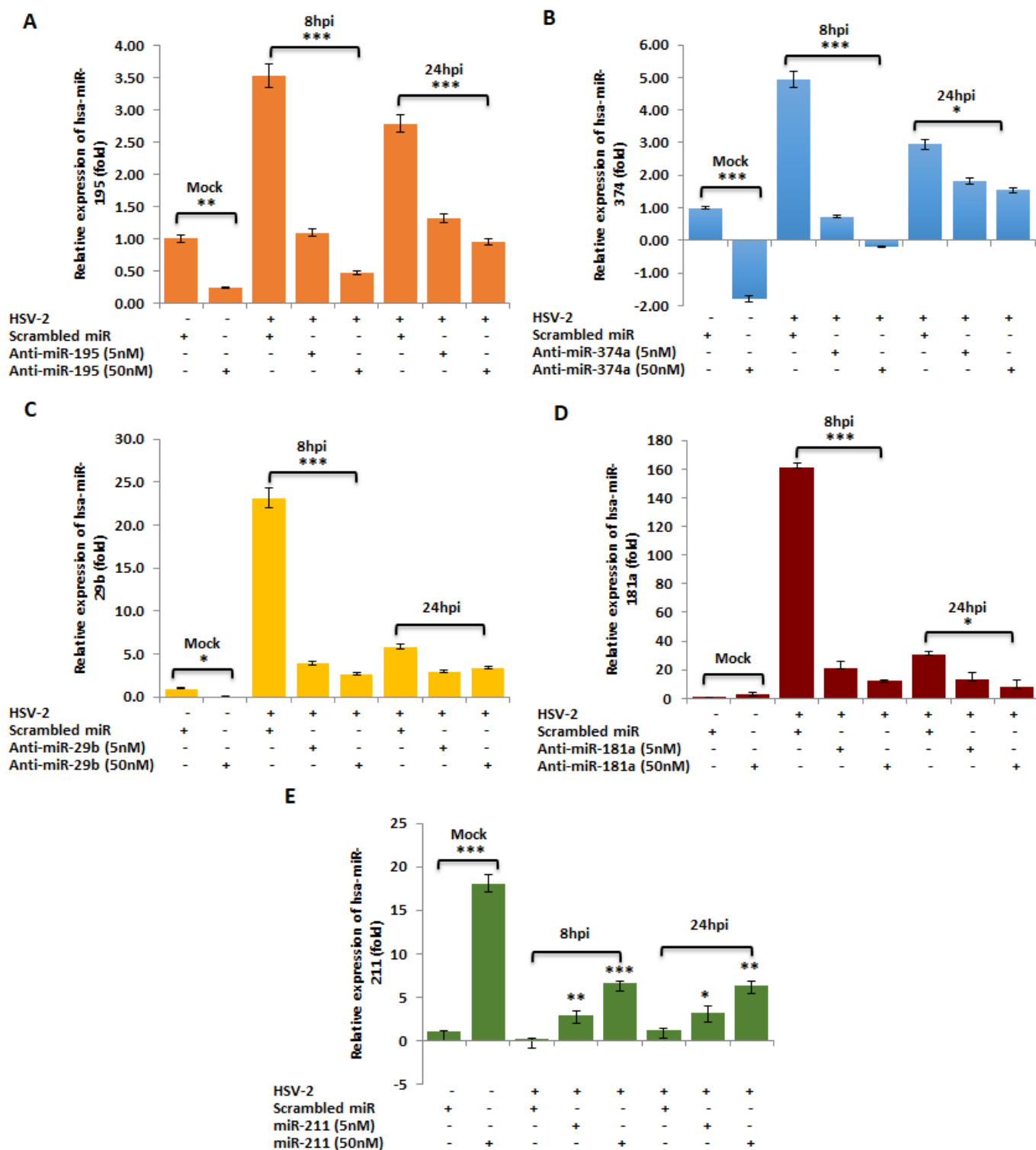
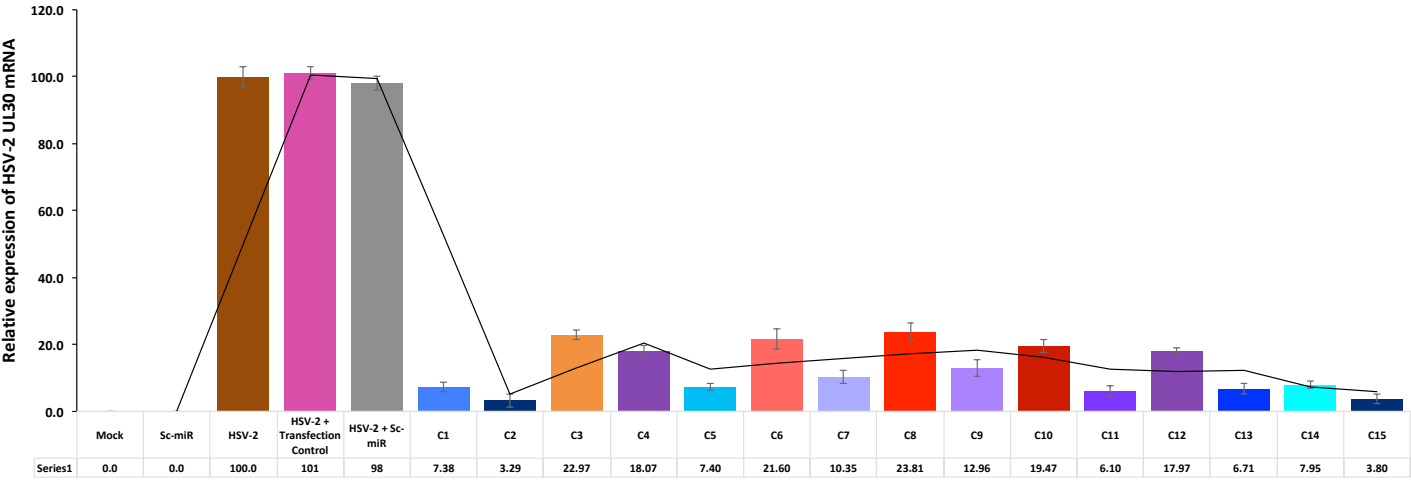


Figure S5

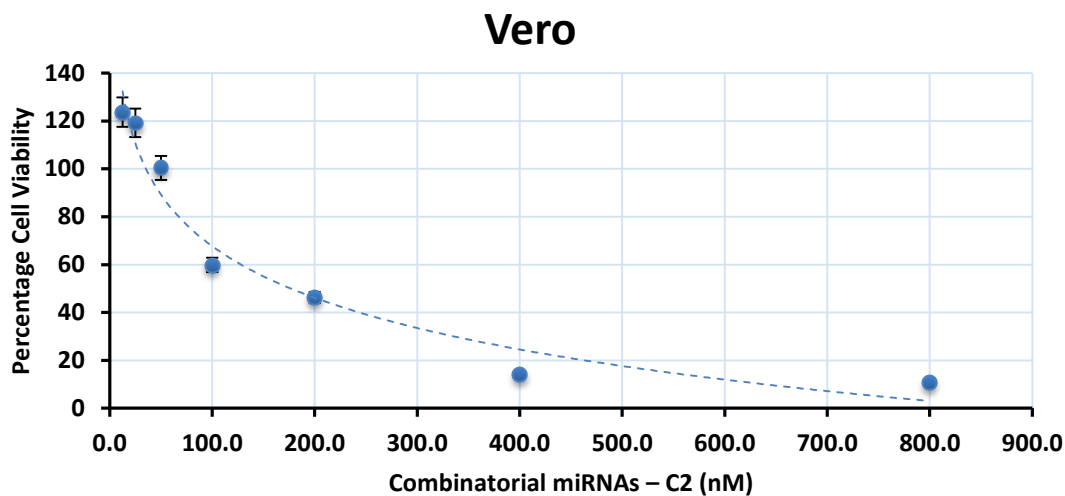
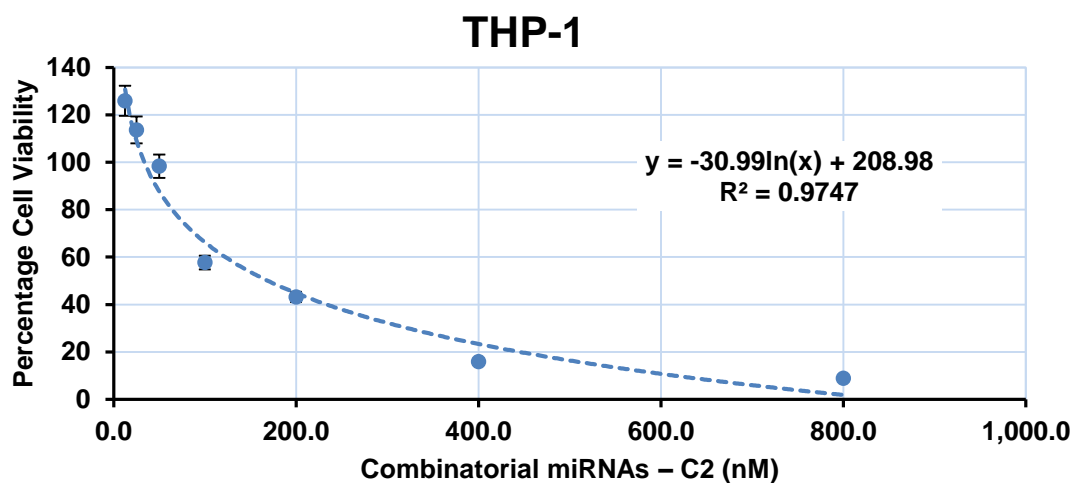
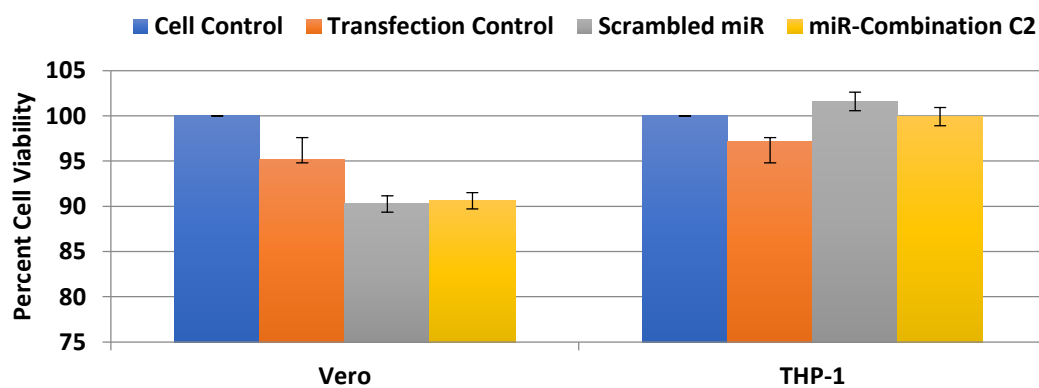
A



B

Combination Name	STD	RUN	Anti-miR-195	Anti-miR-374a	Anti-miR-29b	Anti-miR-181a	mimic-miR-211	Total conc. In combination (nM)	Working Conc.	% Inhibition of HSV-2
C1	14	1	46.44	36.46	15.99	28.37	28.055	155.315	50nM	92.61652181
C2	7	4	32.44	36.46	15.99	41.37	28.055	154.315	50nM	96.70510872
C3	35	7	18.44	36.46	28.99	28.37	41.055	153.315	50nM	77.02890145
C4	26	10	46.44	36.46	28.99	15.37	28.055	155.315	50nM	81.9314074
C5	5	12	32.44	36.46	15.99	15.37	28.055	128.315	50nM	92.60462644
C6	10	14	32.44	49.46	28.99	28.37	15.055	154.315	50nM	78.39562524
C7	3	17	18.44	49.46	28.99	28.37	28.055	153.315	50nM	89.65484778
C8	11	20	32.44	23.46	28.99	28.37	41.055	154.315	50nM	76.1929483
C9	16	22	46.44	36.46	41.99	28.37	28.055	181.315	50nM	87.03932045
C10	6	25	32.44	36.46	41.99	15.37	28.055	154.315	50nM	80.53365204
C11	33	28	18.44	36.46	28.99	28.37	15.055	127.315	50nM	93.90499636
C12	8	30	32.44	36.46	41.99	41.37	28.055	180.315	50nM	82.02954372
C13	20	35	32.44	36.46	28.99	41.37	41.055	180.315	50nM	93.28829546
C14	21	40	32.44	23.46	15.99	28.37	28.055	128.315	50nM	92.04539284
C15	29	42	32.44	36.46	15.99	28.37	15.055	128.315	50nM	96.19967089

Figure S6

A**B****C****Figure S7**

Supplementary Figure Legends: S1-S7

Figure S1: (A) The cellular processes or events associated with the upregulated and the downregulated miRNAs. The upregulated miRNAs in the HSV-2 infected macrophage samples are represented in red colour while downregulated ones are represented in green. Different representations - (B) Scatter plot (C) Volcano plot- of 43 dysregulated miRNAs in the human inflammatory response pathway-focused miRNA microarray assay using Control Vs. HSV-2 infected samples. Red and yellow indicate the upregulated while green and blue represent the downregulated miRNAs in the scatter and volcano plot, respectively. 43 miRNAs were observed to be differentially expressed between the Control and the HSV-2 infected samples at the $P < 0.05$ significance level.

Figure S2: Top ten over-represented pathways associated with (A) targets of the overexpressed miRNAs and (B) targets of the under-expressed miRNA, as per functional enrichment analysis performed against different pathway databases using DAVID.

Figure S3: Gene neighborhood of the selected miRNA targets. (A) STRING Network analysis to reveal the focal point of the target interaction network. The colored nodes represent the miRNA targets and their interactors. Structures within the nodes indicate known 3D structure of their proteins. Different colored edges denote known or predicted interactions from curated databases or are experimentally determined, with fusions, neighborhood, co-occurrence, protein homology or co-expression between them (B-G) First neighbors of each of the miRNA targets. All the network analysis was done using the StringApp in Cytoscape 3.8.2.

Figure S4: (A) String network analysis of the known interactions of AKT1 with other target proteins. (B) miRNet visual analytics platform to represent the interaction network of the targets with other miRNAs and the diseases that may become associated with HSV-2 infection. The green, circular nodes represent the miRNA targets, the blue small, circular nodes represent the miRNAs that are already known to target them and the pink, pentagonal nodes represent the diseases that are linked with HSV-2 infection. The edges in orange represent the interactions between the miRNAs, their targets and the HSV-2 associated diseases.

Figure S5: Transfection efficiencies of the mimic or inhibitors of the miRNAs. (A-D) The fold-change in relative expression of the miRNAs in samples transfected with inhibitors of miR-195, miR-374a, miR-29b or miR-181a at 5nM or 50nM transfected concentrations. (E) The fold-change in relative expression of the miRNAs in samples transfected with the mimic of miR-211 at 5nM or 50nM transfected concentrations.

Figure S6: Representation of *in vitro* validation of the selected 15 miRNA combinations based on the degree of HSV-2 inhibition. Out of the 15 combinations tested for their relative inhibitory effect on the HSV-2 UL30 gene transcription, the highest relative inhibitory effect was observed in the C2 combination (~97%), followed by C15 (~96%), with the lowest inhibition obtained by the combination C8 (~76%), when compared with the HSV-2 infected but untransfected samples or samples without treatment. No change in the UL30 expression was observed upon transfection of transfection control or Scrambled miR followed by HSV-2 infection when compared to the untransfected HSV-2 infected samples.

Figure S7: Cell viability assay by MTT. The effect of different concentrations of the miRNA combination C2 on (A) Vero epithelial cells and (B) differentiated THP-1 cells. (C) The mean CC_{50} value of miRNA combination C2 (Yellow) as determined from three independent assays, in comparison to the different controls used in the assay, i.e. Untransfected cell control (Blue), Transfection control-transfected (Orange) and Scrambled miR-transfected (Grey).